Synthesis, and Structural Investigations of TiO_2 Doped Cr_2O_3 Thin Films for Gas Sensor Applications

Nihad K. Ali[1, a)] and Ikhlas H. Shallal[1, b)]

[1] *Department of Physics, College of Education for Pure Science /Ibn Al-Haitham, Baghdad University, Baghdad, Iraq*

[a)] *Corresponding author: nihad.ali2304@ihcoedu.uobaghdad.edu.iq*
[b)] *akhlas.h.s@ihcoedu.uobaghdad.edu.iq*

Abstract. The most important details of the synthesis by using pulsed laser ablation in deionized water to ablate the Cr_2O_3 and TiO_2 nanoparticles and drop-casting the solutions on the substrates to deposit Cr_2O_3 thin films with concentration ratio (0, 0.2, 0.4, 0.6, 0.8) % of TiO_2 are illustrated. Additionally, a concise and precis explanation of the structural analysis included X-ray diffraction (XRD) and atomic force microscopy (AFM) and gas sensor performance evaluation were provided. (XRD) test revealed that all samples of Cr_2O_3:TiO_2 films have a polycrystalline nature with Rhombohedral structure and the Cr_2O_3 is crystalized as a main plane in (012), while TiO_2 nanoparticles have anatase phase with tetragonal crystal structure at plane (112). The gas sensor device of the heterojunction of Cr_2O_3:TiO_2/Psi with concentration ratio (0, 0.2, 0.4, 0.6, 0.8) % of TiO_2 were examined when exposed to 400ppm of NO_2 gas at various temperatures (R.T, 100, 150) °C. The maximum value of sensitivity was 475.11% detected at 0.6% TiO_2 at operation temperature of 100°C.

Keywords: thin films, Structural, gas sensing, Cr_2O_3:TiO_2, laser ablation.

INTRODUCTION

In recent years, discussions regarding metal oxide semiconductors (MOs) have dominated research, due to them distinct optical, magnetic, and electrical characteristics [1]. As with all oxides of metal, chromium (III) oxide has critically influenced academic dialogue either a nano-powder or thin film [2]. Chrome oxides like CrO_2 and Cr_2O_3 and chromium (Cr)–titanium (Ti) interaction types, have several states according to the applied power on the chromium metallic phase and shows peaks with high energy due to its significant intrinsic characteristics. In the last two decades the most transition oxide that had been studied is titanium oxide which is required in many areas of applications like solar cells, gas sensors and transparent electrodes [3]. Because of Cr_2O_3 diverse properties, it falls under the most stable phases and the hardest transition MOs which enabled it to be a unique industrial material [4]. Where it has a high melting point (2473K), resistance the oxidation at elevated temperatures, and large optical absorbance [5]. Chromium trioxide (Cr_2O_3), is a p-type semiconductor with a wide optical energy gap, excess oxygen, and a refractive index with a high value [6]. In this regard, titanium dioxide (TiO_2) also known as an MOs with high refractive index, photocatalytic efficiency, and chemical stability [7], both Cr_2O_3 and TiO_2 are employed as thin films and sensing species in gas sensors according to their properties and advantages of low cost, tiny size and operation at ease and good ability to reverse and long life, good and reliability for real-time applications when compared with other gas sensing devices. [8]. The substantial mechanism of gas sensors based on metal oxide semiconductor thin films depends on electrical resistance that changes during the interaction between the sensor's material surface and the molecules of the absorbed gas, overall, two functions occur in chemical sensors, firstly receptor function to detect and distinguish the gas, secondly transducer function to obtain output signal from the chemical signal [9]. Various techniques were utilized for producing gas sensor thin films. As Thermal evaporation [10], sol-gel [11], spin-coating [12], pulsed laser deposition (PLD) [13,14] R.F magnetron sputtering [15], spray pyrolysis [16,17] and hydrothermal method [18].

This work aims to investigate the effect of adding TiO_2 dopant to Cr_2O_3 nanoparticles deposited by implemented pulsed laser ablation in liquid (PLAL) and drop-casting techniques to explore the structural and gas sensing properties.

EXPERIMENTAL TECHNIQUES

To ablate the nanoparticles (NP_S) of the chromium trioxide (Cr_2O_3) and titanium dioxide (TiO_2) via pulse laser ablation in liquid (PLAL). First, High purity powders with purity (99.999%) which were supplied by (Central Drug House, India) company and (Sigma –Aldrich, China) company respectively were weighed as 7g of Cr_2O_3 and 2g of TiO_2. Then, they were compacted by the hydraulic compressor under a pressure of 12 Ton with a duration of 24 hours to create pellets with a diameter of 1.7cm. The pellet was placed at the bottom of a glass beaker that contains 20ml of deionized water and it was irradiated by Nd:YAG pulsed laser type (Huafei) with 1064nm wavelength and laser energy of 600mJ for 500 pulses , pulses frequency 8Hz . A converging lens of 10cm focal length was used to focus the laser beam as a spot with a diameter of 2.3mm on the target surface, After the continuing of the ablation process and rotating the beaker, a colloidal solution was prepared, To synthesis the doped thin films, the colloidal solutions with volume of Cr_2O_3 (9.98 , 9.96 , 9.94 , 9.92)ml and TiO_2 with (0.02 , 0.04, 0.06 , 0.08)ml were sequentially mixed, The drop casting method was used to deposit films by dropping 1ml of each colloidal solution on a glass and n-type porous silicon substrates with dimensions of $(1.5\times1.5)cm^2$ at a temperature of 400℃, the liquid evaporates by the heating effect to form the thin film with thickness 200nm. Structural and sensitivity measurements were recorded for Cr_2O_3 films doped with (0.2, 0.4, 0.6, 0.8) % of TiO_2 ratios. X-ray diffraction analysis technique model PHILIPS PW 1730, The Netherland, Cu-Kα radiation (λ=1.54060nm) operated on a tube voltage of 40KV and current of 30A was employed to characterize the crystalline structure for the prepared films, the scan angle was changed within the range from 10deg to 80deg with a step size of 0.05deg, The morphology of thin films surface was studied by atomic force microscopy (TT-2 AFM Workshop, USA.). Gas-sensing measurements which included, the resistance of thin films in the presence of NO_2 gas with a concentration of 400ppm, The NO_2 gas sensitivity, response, and recovery times of the samples were calculated and discussed. Figure 1. illustrates a simple diagram of the experimental (PLAL system).

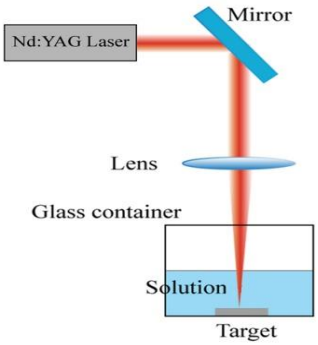

FIGURE 1. Pulsed laser ablation in liquid system.

RESULTS AND DISCUSSION

Structural characterization

The structural characterization of the prepared thin films was studied using the results of x-ray diffraction (XRD) and atomic force microscopy (AFM) analyses.

X-ray diffraction spectrum

The x-ray diffraction spectrum was employed to characterize the crystallographic features of the as-deposited

thin films. Debye Scherrer's equation was utilized to compute the crystallite sizes in nm [19]:

$$Crystalline\ size\ (C.s) = \frac{(0.94)\lambda}{\beta COS\theta} \quad (1)$$

where (0.94) is the Scherer's constant, λ is the X-ray wavelength in nm, and the full width at half maximum (FWHM) is symbolized as β in radian.The pure and doped Cr_2O_3 thin films yielded a polycrystalline nature and the Cr_2O_3 is crystalized as Rhombohedral structure according to ICDD card NO. 00-006-0504, with a main phase in plane (012) corresponding to $2\theta = 24.543^o$ and the plane (202) in the concentration (0.4% and 0.6%) which belongs to TiO_2 corresponding to $2\theta = 44.143^o$,and 44.193^o respectively. The secondary phase CrO_3 with orthorhombic structure was surfaced at the concentration (0% , 0.2% , 0.4% , 0.6%) of TiO_2 in the plan (200) based on ICDD card NO. 00-032-6285 , May be the appearance of the secondary phase was the deposition conditions where the redox behavior was foreseen [20] , A new peak was observed in (0.8%) TiO_2 thin film at plane (112) and $2\theta = 38.593^o$ indicates the dopant TiO_2 Anatase phase with tetragonal crystal system compared with ICDD card NO. 21-1272 ,The nanoparticles of Cr_2O_3 crystalline size where decreased along (012)plane ,with increasing TiO_2 concentration from 33.66 nm for 0.2% TiO_2 to 21.69nm for 0.8% TiO_2 and the same behavior at plane (202) was decreased from 21.04 nm for the sample of 0.4% TiO_2 to 20.79nm for 0.6% TiO_2, the increasing of TiO_2 dopant concentration ratio influenced by decreasing peaks intensity this might be due to the existence Ti^{4+} ions in Cr_2O_3 lattice and substitute Cr^{3+} ions [21]. Figure 2. illustrates XRD patterns of pure and doped Cr_2O_3 thin films.

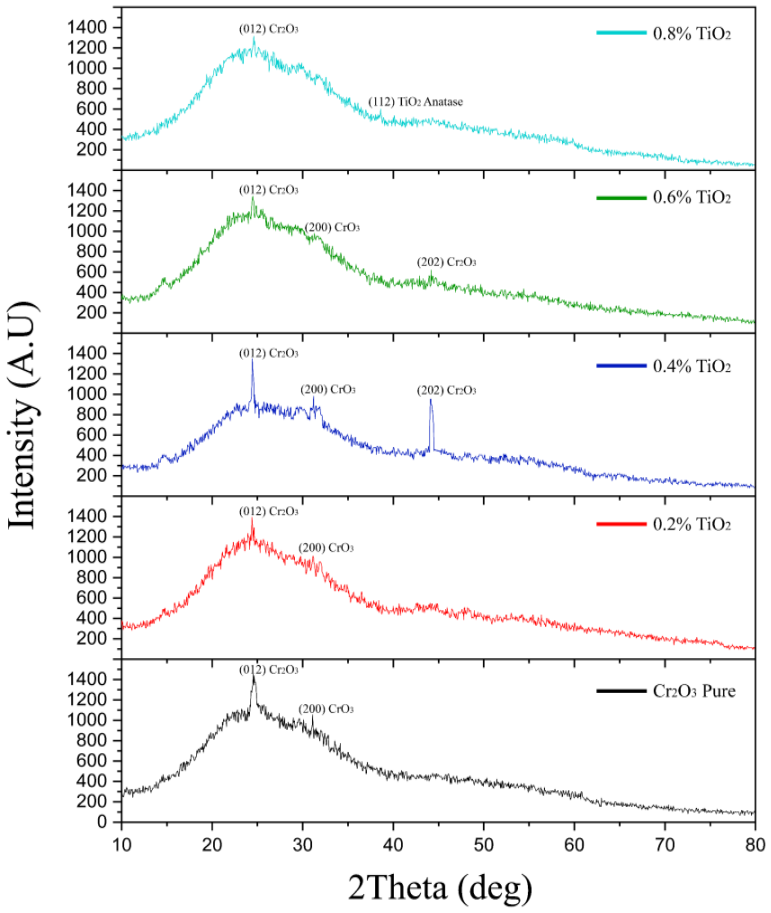

FIGURE 2. XRD pattern of pure and doped Cr_2O_3 thin films.

ATOMIC FORCE MICROSCOPY (AFM)

The morphology of deposited thin films and surface roughness was detected by AFM 3D images fig. 3. which clearly shows granular topography, where granular nanostructures have high surface area which provides more interaction sites with gas molecules and as a result the gas sensitivity increases with a proportional relationship [22], the pure Cr_2O_3 thin film exhibited the lowest grain size (30.16nm) which shows an inconsistent increase in the doped Cr_2O_3 thin film relative to the pure Cr_2O_3 thin film with increasing the ratio of TiO_2 dopant (0.2 % , 0.4 % , 0.6% , 0.8 %) , the grain size increased to 77.10nm after doping with ratio of 0.2 % TiO_2 followed by decrease in values of 48.79nm and 42.78nm in ratio of 0.4% and 0.6% TiO_2 respectively , the reason might be the scattering of grain boundaries resulting from crystalline degradation of thin films [23] , and increase to 85.02nm at ratio 0.8% TiO_2. The doped sample with ratio 0.2% showed the highest value of mean roughness of 19.65nm and root mean square (RMS) of 27.12nm and the 0.8% TiO_2 doped thin film recorded mean roughness of 10.92nm and RMS of 15.03nm. Table 1. represents the AFM parameters for pure and doped Cr_2O_3 thin films. The reason of the increase in roughness might be due to the random distribution of the faceted hillocks on the relatively smooth structure and densification of the deposition procedures [24].

TABLE 1. AFM parameters for pure and doped Cr_2O_3 thin films.

Sample	RMS (nm)	Mean Roughness (nm)	Average Grain Size (nm)
Cr_2O_3/PSi	10.20	8.61	30.16
Cr_2O_3: (0.2%)TiO_2/PSi	27.12	19.65	77.10
Cr_2O_3: (0.4%)TiO_2/Psi	10.00	7.86	48.79
Cr_2O_3: (0.6%) TiO_2/Psi	10.14	7.99	42.78
Cr_2O_3: (0.8%)TiO_2/PSi	15.03	10.92	85.02

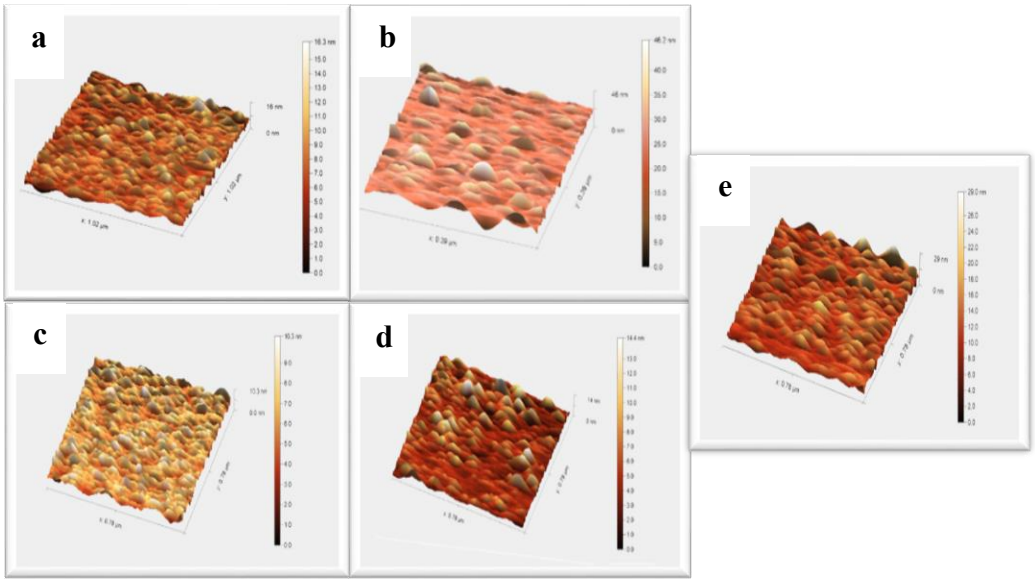

FIGURE 3. AFM images for pure and doped Cr_2O_3 thin films.
a) 0% TiO_2 b) 0.2% TiO_2 c) 0.4% TiO_2 d) 0.6% TiO_2 e) 0.8% TiO_2

GAS SENSOR PROPERTIES

The gas sensor device prepared from the heterojunction of Cr_2O_3:TiO_2/Psi with concentration ratio (0 , 0.2 , 0.4 , 0.6 , 0.8)% of TiO_2 were examined when exposed to 400ppm of NO_2 gas at various temperatures (R.T , 100 , 150)°C , the resistance for as-sensors where decrease when exposed to NO_2 oxidizing gas as a typical behavior of P-type semiconductor nature due to the increasing of the positive holes concentration as a result for introduction the negative charge of adsorbed oxygen ions and the molecules of the targeted gas [25,26] , as shown in figs. 4 and 5.

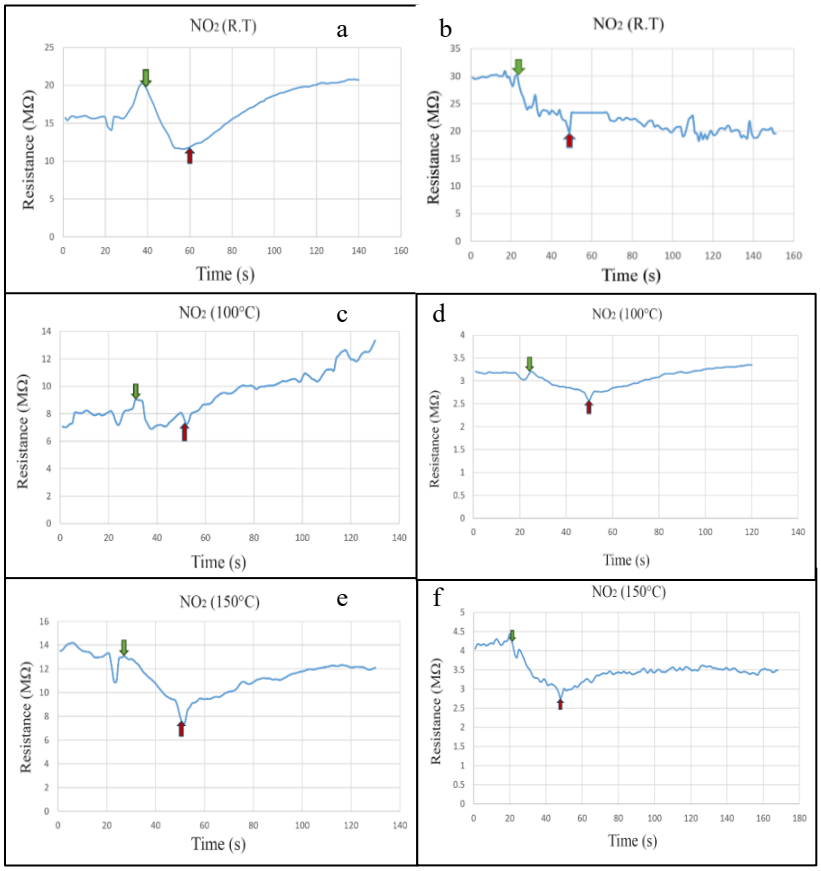

FIGURE 4a,b,c,d,e,f. Resistance variation with time of thin films in three different operation temperatures for:
I - Pure Cr_2O_3 II - Cr_2O_3:(0.2%) TiO_2

Table (2) shows the sensitivity behavior that increases from 51.60 % to 158.80% when concentration ratio of TiO2 was increased from 0% to 0.4% in a different operation temperature. it might be the doping effect of metal oxide layer with other metal oxide which enhances the sensing characteristics [27].

The maximum value of sensitivity was 475.11% detected at 0.6% TiO_2 at operation temperature of 100°C, it could be the synergistic effect of heterojunction where the gas molecules react with adsorbed oxygen ions in first material of the junction and the by-product may readily react with the oxygen ions in the second material to complete the reaction [28]. Figure 6. clarify the variation of sensitivity for NO_2 as a function to the TiO_2 dopant ratio.

Doping with elements can affect the surface defects and electrical properties of the sensor material, enhancing electron transfer. At the same time, doping with elements can alter the band gap of the material, thereby improving its gas sensitivity. In particular, doping with metals with high catalytic activity and low Fermi levels will stimulate electronic and chemical sensing, effectively improving the material's gas sensitivity [29]. formed titanium dioxide nanofiber films doped with palladium with varying amounts of doping using a flame surface stabilization (FSRS) technique. It

was found that doping with noble metals enhanced the response intensity of the titanium dioxide-based sensor to carbon monoxide gas, while also significantly reducing its response/recovery times to ammonia gas [30].

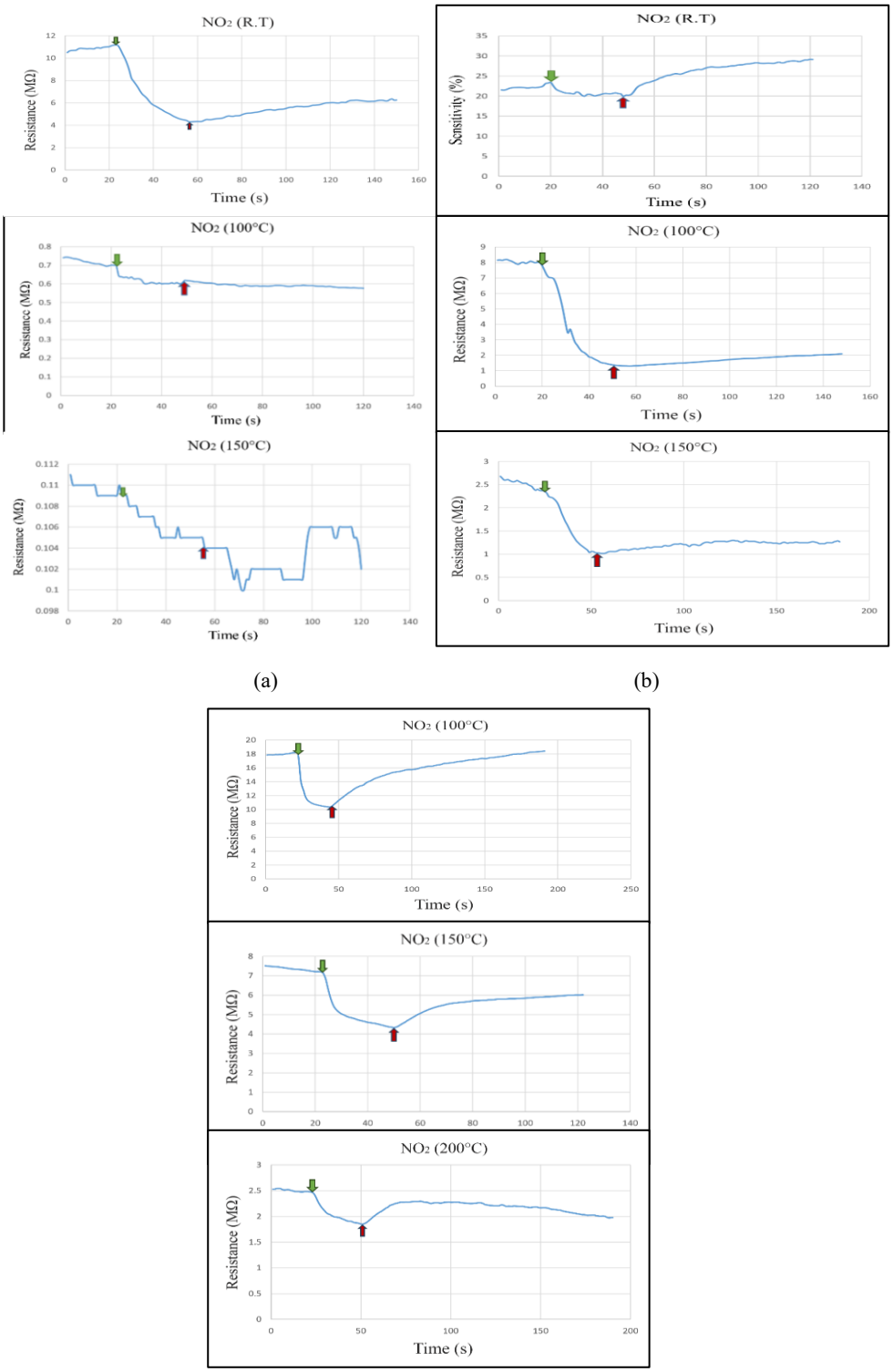

FIGURE 5. resistance variation with time of thin films in three different operation temperature for:
a- Cr_2O_3:(0.4%) TiO_2 b - Cr_2O_3:(0.6%) TiO_2 c - Cr_2O_3:(0.8%) TiO_2

TABLE 2. Sensitivity characteristics of Cr_2O_3:TiO_2/PSi at different operation temperature.

Sample	Operating Temp.(℃)	Sensitivity (%)	Response Time (s)	Recovery Time (s)
Cr_2O_3/PSi	R.T	51.60	23.4	90.9
	100	23.26	21.6	63
	150	50.00	25.2	45.9
Cr_2O_3: (0.2%)TiO_2/PSi	R.T	67.00	18.9	81
	100	24.24	18.9	61.2
	150	72.99	23.4	61.2
Cr_2O_3: (0.4%)TiO_2/PSi	R.T	158.80	29.7	84.6
	100	12.78	25.2	45
	150	4.81	30.6	39.6
Cr_2O_3: (0.6%) TiO_2/PSi	R.T	17.46	25.2	64.8
	100	475.11	27.9	62.1
	150	125.96	24.3	61.2
Cr_2O_3: (0.8%)TiO_2/PSi	100	75.34	19.8	68.4
	150	66.51	25.2	45
	200	33.87	27	44.1

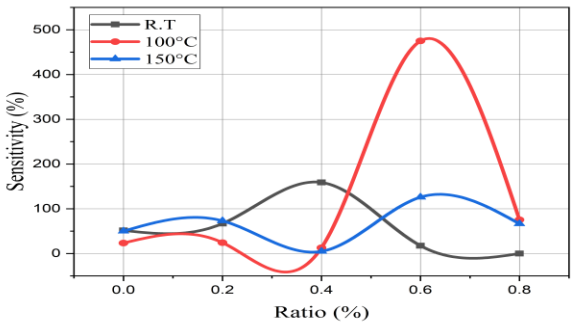

FIGURE 6. shows the variation of sensitivity for NO_2 as a function of dopant ratio.

The sample doped by 0.8% TiO_2 didn't show a sensitivity for NO_2 gas at room temperature but detected a good value of sensitivity (75.34%) at 100°C , the response time and recovery time changed in different values relative to TiO_2 concentration in thin films but recorded the lowest response time magnitude (18.9s) at 0.2% TiO_2 concentration thin film at both room temperature and 100°C, while the minimum recovery time was 39.6s for the sample with concentration of 0.4% TiO_2 at 150°C.

CONCLUSIONS

Cr_2O_3 thin films pure and doped by TiO_2 with contained ratio (0 , 0.2 , 0.4 , 0.6 , 0.8)% were synthesized by using pulsed laser ablation in liquid and drop-casting processes step by step. X-ray diffraction (XRD), revealed that all samples of Cr_2O_3:TiO_2 films have a polycrystalline nature with Rhombohedral structure with main plane in (012),while TiO_2 nanoparticles have Anatase phase with tetragonal crystal structure. The maximum sensitivity value of gas sensor device of Cr_2O_3: 0.6% TiO_2/Psi for NO_2 gas was 475.11% detected at operation temperature of 100°C. The high performance of as fabricated gas sensor indicated that it is promising for NO_2 sensitivity toward air quality

which make it a good candidate for investment in environmental monitoring and industrial gasses hazards trucker also it can be utilized in cross-sensitivity tests.

ACKNOWLEDGEMENTS

The authors extend their sincere gratitude to the Department of Physics at the College of Education for Pure Science/Ibn Al-Haithem, University of Baghdad for their support. We also deeply appreciate to dr. morooj A. Aboode\Solar Energy Research Center, Renewable Energy Directorate\Iraq, for her assistance.

REFERENCES

1. M. H. Suhail, I. K. Adehmash, S. M. Abdul Kareem, D. A. Tahir, and O. G. Abdullah, *Trans. Electr. Electron. Mater.* **21**, 327 (2020).
2. A. Zekaik, H. Benhebal, and B. Benrabah, *High Temp. Mater. Proc.* **38**, 806 (2019).
3. A. Hajjaji, M. Amlouk, M. Gaidi, B. Bessais, and M. A. El Khakani, Chromium Doped TiO_2 Sputtered Thin Films: Synthesis, Physical Investigations and Applications (Springer, Cham, 2015).
4. A. Kadari, T. Schemme, D. Kadri, and J. Wollschläger, *Results Phys.* **7**, 3124 (2017).
5. A. K. Panda, A. Singh, R. Divakar, N. G. Krishna, V. R. Reddy, and R. Thirumurugesan, *Thin Solid Films* **660**, 328 (2018).
6. J. Singh, V. Verma, R. Kumar, and R. Kumar, *Mater. Res. Express* **6**, 096414 (2019).
7. H. Chen, B. A. Prastika, Z. Zhang, and C. Zhang, *Appl. Phys. A* **131**, 134 (2025).
8. J. Cao, Y. Xu, L. Sui, X. Zhang, S. Gao, and X. Cheng, *Sens. Actuators B Chem.* **220**, 1146 (2015).
9. S. Ponmudi, R. Sivakumar, C. Sanjeeviraja, C. Gopalakrishnan, and K. Jeyadheepan, *Appl. Surf. Sci.* **463**, 556 (2019).
10. S. H. Salman, N. A. Hassan, and G. S. Ahmed, *Chalcogenide Lett.* **19**, 125 (2022).
11. S. A. Kadhim and T. M. Al-Saadi, *Ibn Al-Haitham J. Pure Appl. Sci.* **36**, 159 (2023).
12. I. A. Kareem and H. F. Oleiwi, *Ibn Al-Haitham J. Pure Appl. Sci.* **36**, 137 (2023).
13. M. A. Abood and B. A. Hasan, *Iraqi J. Sci.* **64**, 1675 (2023).
14. A. J. Haider, R. H. Al-Anbari, G. R. Kadhim, and C. T. Salame, "Exploring potential environmental applications of TiO_2 nanoparticles," Energy Procedia 119, 332–345 (2017).
15. S. H. Salman, A. A. Shihab, and A. K. Elttayef, *Energy Procedia* **157**, 283 (2019).
16. Q. G. Al-zaidi, A. M. Suhail, and W. R. Al-azawi, *Appl. Phys. Res.* **3**, 89 (2011).
17. A. H. A. Alrazak, S. H. Salman, I. A. Abbas, M. H. Mustafa, H. M. Ali, and S. A. Abbas, *Dig. J. Nanomater. Biostruct.* **20**, 191 (2025).
18. S. A. Hamdan and I. M. Ali, *Baghdad Sci. J.* **16**, 0221 (2019).
19. S. S. Mahmood, B. A. Hasan, and A. F. Rauuf, *Iraqi J. Sci.* **65**, 3754 (2024).
20. V. B. Kamble and A. M. Umarji, *J. Mater. Chem. C* **1**, 8167 (2013).
21. T. C. Kaspar, P. V. Sushko, M. E. Bowden, S. M. Heald, A. Papadogianni, and C. Tschammer, *Phys. Rev. B* **94**, 155409 (2016).
22. N. G. Deshpande, Y. G. Gudage, R. Sharma, J. C. Vyas, J. B. Kim, and Y. P. Lee, "Studies on tin oxide-intercalated polyaniline nanocomposite for ammonia gas sensing applications," *Sensors and Actuators B: Chemical* **138**, 76 (2009).
23. N. Manjula, M. Pugalenthi, V. S. Nagarethinam, K. Usharani, and A. R. Balu, *Mater. Sci.-Pol.* **33**, 774 (2015).
24. S. M. Abdulkareem, M. H. Suhail, and I. K. Adehmash, *Iraqi J. Sci.* **62**, 2176 (2021).
25. F. El Haj Hassan, S. Moussawi, W. Noun, C. Salame, and A. V. Postnikov, "Theoretical calculations of the high-pressure phases of SnO_2," Comput. Mater. Sci. 72, 86–92 (2013).
26. Aleabi, S.H., Watan, A.W., Salman, E.M.-T., kareem Jasim A.,Shaban, A.H., Alsaadi, T.M., AIP Conference Proceedings, 2018, 1968, 020019.
27. N. Dasgupta, S. Ranjan, and E. Lichtfouse, eds., *Environmental Nanotechnology Volume 3* (Springer, 2020).
28. M. K. Jayaraj, ed., Nanostructured Metal Oxides and Devices: Optical and Electrical Properties (Springer, Singapore, 2020).
29. Ahmed BA, Mohammed JS, Fadhil RN, Shaban AH, Al Dulaimi AH. *Chalcogenide Lett*. 2022;19(4):301-308.
30. Salman SH, Jahil SS, Hassan NA, Abbas SA, Jasim KA. Ammonia gas sensing using porous silicon. *J Phys Conf Ser*. 2024;2857(1):012051